EDGEWOOD CHEMICAL BIOLOGICAL CENTER
U.S. ARMY RESEARCH, DEVELOPMENT AND ENGINEERING COMMAND
Aberdeen Proving Ground, MD 21010-5424

ECBC-CR-135

VAPOR PRESSURE DATA ANALYSIS AND CORRELATION METHODOLOGY FOR DATA SPANNING THE MELTING POINT

David E. Tevault

JOINT RESEARCH AND DEVELOPMENT, INC.
Stafford, VA 22556-8615

October 2013

Approved for public release; distribution is unlimited.

U.S. ARMY
RDECOM

Disclaimer

REPORT DOCUMENTATION PAGE

Form Approved
OMB No. 0704-0188

1. REPORT DATE *(DD-MM-YYYY)*
XX-10-2013

2. REPORT TYPE
Final

3. DATES COVERED *(From - To)*
Mar 2013 - June 2013

4. TITLE AND SUBTITLE
Vapor Pressure Data Analysis and Correlation Methodology for Data Spanning the Melting Point

5a. CONTRACT NUMBER
SPO0700-00-D-3180/338493

5b. GRANT NUMBER

5c. PROGRAM ELEMENT NUMBER

6. AUTHOR(S)
Tevault, David E. (JRAD, Inc.)

5d. PROJECT NUMBER
DO CB12-0363

5e. TASK NUMBER

5f. WORK UNIT NUMBER

7. PERFORMING ORGANIZATION NAME(S) AND ADDRESS(ES)
Joint Research and Development, Inc.
50 Tech Parkway, Suite 209, Stafford, VA 22556-8615

8. PERFORMING ORGANIZATION REPORT NUMBER
ECBC-CR-135

9. SPONSORING/MONITORING AGENCY NAME(S) AND ADDRESS(ES)
Defense Threat Reduction Agency, 8725 John J. Kingman Road, MSC 6201, Fort Belvoir, VA 22060-6201

10. SPONSOR/MONITOR'S ACRONYM(S)
DTRA

11. SPONSOR/MONITOR'S REPORT NUMBER(S)

12. DISTRIBUTION / AVAILABILITY STATEMENT
Approved for public release; distribution is unlimited.

13. SUPPLEMENTARY NOTES
COR: Joseph Williams

14. ABSTRACT

Vapor pressure information is important for a number of reasons related to chemical and biological warfare defense applications. Since it is often impractical to measure data over the desired range of temperatures, it becomes very useful to develop correlations based on measured data to facilitate interpolation and extrapolation. Penski reported a detailed description of one method commonly used to correlate vapor pressure data. This report expands on that work by exploring the merits of a similar metric to correlate the experimental data. A problem that has arisen involves data that extends across the melting point of the analyte. This phenomenon has been observed for a number of compounds of interest recently, and the data can be difficult to correlate, particularly when liquid and solid phase data are recorded using different analytical methods. We present here a method to quantitatively correlate such data sets.

15. SUBJECT TERMS

Antoine equation correlation
Clausius-Clapeyron correlation
Vapor pressure
Log-difference analysis
Chemical warfare agent
Log-difference squared analysis
Melting point

16. SECURITY CLASSIFICATION OF:			**17. LIMITATION OF ABSTRACT**	**18. NUMBER OF PAGES**	**19a. NAME OF RESPONSIBLE PERSON**
					David E. Tevault
a. REPORT	**b. ABSTRACT**	**c. THIS PAGE**			**19b. TELEPHONE NUMBER** *(include area code)*
U	U	U	UU	28	(410) 436-3860

Blank

PREFACE

The work described in this report was authorized under project no. DO CB12-0363. The work was started in March 2013 and completed in June 2013.

The use of either trade or manufacturers' names in this report does not constitute an official endorsement of any commercial products. This report may not be cited for purposes of advertisement.

This report has been approved for public release.

Acknowledgments

The author acknowledges Ann Brozena, U.S. Army Edgewood Chemical Biological Center, for her interest in this work, critical review, and helpful suggestions.

Blank

CONTENTS

Figures

Tables

VAPOR PRESSURE DATA ANALYSIS AND CORRELATION METHODOLOGY FOR DATA SPANNING THE MELTING POINT

1. INTRODUCTION

The vapor pressure of chemical warfare agents is closely related to persistence and whether a material represents a vapor threat to unprotected personnel. In addition, generation of vapor streams for testing of protection and detection equipment and inhalation toxicology requires a quantitative knowledge of the vapor-liquid equilibrium of these materials as a function of temperature. As a result, U. S. Army Edgewood Chemical Biological Center (ECBC) has maintained considerable interest and technical capability in the measurement of physical property data, including vapor pressure, for many decades. In the past, complementary experimental methods of principal interest used to measure vapor pressure included Knudsen effusion, differential thermal analysis (DTA), and isoteniscope.[1-3]

Knudsen effusion is usually performed at low pressures by precise measurement of the rate of mass loss of a material through an orifice of known area under vacuum inside a specially designed cell at a known temperature. This method requires the availability of a high-purity analyte material, which can be particularly difficult for materials of interest in chemical and biological defense applications. Another technical difficulty with the Knudsen effusion method is the inability to analyze the effusing specimen. If the effusing molecules are associated or conjugate species, the associated calculations will be adversely affected.

DTA is performed by heating a sample contained in a glass capillary into which a thermocouple has been inserted at a fixed pressure and measuring the temperature difference between the specimen and a reference thermocouple embedded in glass beads in a second capillary tube. The temperature difference is ascribed to vaporization of the sample from the capillary at the boiling point, and data analysis provides the boiling temperature at the specified pressure, that is, a reduced pressure boiling point for that material. DTA is restricted to higher temperatures and pressures (above about 200 Pa) and also requires access to a pure specimen.

The isoteniscope is a glass apparatus consisting of a reservoir to hold the specimen and an internal U-tube connected to an external manometer. After the specimen is adequately degassed, the liquid menisci in the U-tube are brought to the same level and the pressure read on the manometer. The measurement is straightforward but the sample size required is relatively large, typically exceeding 10 grams, which is undesirable when working with chemical warfare agents.

More recent work has focused on a thermal analysis technique related to DTA, that is, differential scanning calorimetry (DSC). DSC is used for measuring data at high temperature and vapor saturation (or transpiration) at ambient temperatures. DSC work at ECBC closely follows the method prescribed by the American Society for Testing and Materials (ASTM) International.[4] However, this method has been modified in order to extend the lower end of the range of applicability from the recommended 5 kPa to as low as 0.2 kPa.[5,6]

Vapor saturation is also a variation of an accepted ASTM method[7] and has been modified at ECBC to accommodate materials with a wide variety of volatilities, including the nerve agents sarin[8] (GB) and VX.[9] Vapor pressure data for higher volatility materials[8,10,11] have been determined by simply measuring mass loss after purging a specially designed sample container. This version of the gravimetric method assumes no association of the evaporating species and is only useful for high-purity materials since the purged vapor is not analyzed. The measured data are converted to vapor pressure assuming ideal gas behavior. Quantitative analysis of the effluent by gas chromatography (GC) using direct injection of a known volume of effluent[12] or a trap-and-purge method has been used for less volatile materials[9] and has the distinct advantage of being applicable to impure samples since the GC separates the components of the mixture prior to performing quantitative measurements. Other analysis methods, such as liquid chromatography-mass spectrometry, which may be particularly suitable for extremely low-volatility and thermally labile materials, are currently under investigation.

In this report, we review the work of Penski by examining in detail the advantages and disadvantages of two commonly applied metrics for correlating experimental data.[13] The metric used by Penski is the square of the difference in the logarithms of measured and correlated values. This analysis provides a result that is indistinguishable from a linear least squares treatment. A second method analyzed in detail is performed by minimizing the sum of the absolute values of the differences between the logarithms of the experimental and correlated values. The utility of a third metric based on difference between experimental and correlated data values squared is briefly addressed, also.

These metrics have been compared by analyzing three test data sets consisting of nine calculated data points each. Each artificial data set was modified by changing one data point in each set so it does not fit the pattern of the others: the first towards the high end of the temperature range, the second, in the middle, and the third towards the low end of the temperature range. These synthetic data sets are listed in Tables 1, 2, and 3, respectively. Our starting point for the accompanying analysis is the Antoine equation shown as eq 1.[14]

It has recently come to our attention that data measured on either side of the melting point for materials of interest[15,16] need to be treated in a quantitative manner, and the methodology used to do so was not elaborated in Penski's reports. We describe a methodology to treat such data herein.

2. PROCEDURE

Three test data sets have been constructed based on the hypothetical Antoine equation shown in eq 1. The first was altered by imposing an outlier data point in the high temperature range, shown in Table 1, the second with an outlier data point in the middle temperature range, shown in Table 2, and the third with an outlier data point in the low temperature range, shown in Table 3.

$$\ln(\mathrm{VP/Pa}) = a - b/(c + \mathrm{T_K}) = (22.0000 - 5000.00/(\mathrm{T_K} - 50.0000)) \qquad (1)$$

where ln(VP/Pa) is the natural logarithm of the vapor pressure value in Pascal units, *a*, *b*, and *c* are Antoine equation correlation constants, and T_K is absolute temperature in Kelvin.
The Antoine constants in eq 1 are similar to the constants reported for a variety of analytes, particularly a series of nerve agent simulants.[11] Several observations, or rules of thumb, related to the effects of changing the Antoine constants have been useful in the present work. These include the following:

- Increasing the Antoine equation *a* constant moves calculated vapor pressure values up on the standard plot of ln(VP) versus reciprocal absolute temperature. Decreasing the Antoine equation *a* constant moves calculated vapor pressure values down on the standard plot.
- Increasing the *b* constant reduces the calculated vapor pressure values and causes the slope of the standard plot to become steeper (more negative).
- The *c* value depends on the range of temperatures investigated and data scatter. For narrow temperature ranges, *c* may be zero, corresponding to a Clausius-Clapeyron equation. In this case, the standard plot (logarithm of vapor pressure versus reciprocal temperature) is a straight line. Usually, *c* values for extended data sets range between -40 and -80.
- Positive *c* values are rejected on thermodynamic grounds, since a positive ***c*** value results in the standard plot having a positive curvature and the heat of vaporization decreasing with increasing temperature.
- In cases where there is no significant difference between correlations derived using two (Clausius-Clapeyron equation) or three (Antoine equation) fit constants, we report the two-parameter correlation.

Table 1. Test Vapor Pressure Data Set with High-Temperature Outlier **(Bold Font)**

Temperature/ºC	Temperature/K	VP_{expt}/Pa	VP_{calc}/Pa‡	Percent Difference*
0	273.15	0.6660	0.6660	0.00
20	293.15	4.206	4.206	0.00
40	313.15	20.07	20.07	0.00
60	333.15	76.82	76.82	0.00
80	353.15	246.3	246.3	0.00
100	373.15	683.6	683.6	0.00
125	398.15	2076	2076	0.00
150	423.15	5435	5435	0.00
175	**448.15**	**6302**	**12606**	**–50.01**
200	473.15	26472	26472	0.00

*100 • (VP_{expt} – VP_{calc})/VP_{calc}
‡Based on eq 1

Table 2. Test Vapor Pressure Data Set with Mid-Temperature Outlier **(Bold Font)**

Temperature/°C	Temperature/K	VP_{expt}/Pa	VP_{calc}/Pa‡	Percent Difference*
0	273.15	0.6660	0.6660	0.00
20	293.15	4.206	4.206	0.00
40	313.15	20.07	20.07	0.00
60	333.15	76.82	76.82	0.00
80	353.15	246.3	246.3	0.00
100	**373.15**	**341.7**	**683.6**	**–50.01**
125	398.15	2076	2076	0.00
150	423.15	5435	5435	0.00
175	448.15	12610	12610	0.00
200	473.15	26470	26470	0.00

*100 • $(VP_{expt}-VP_{calc})/VP_{calc}$
‡Based on eq 1

Table 3. Test Vapor Pressure Data Set with Low-Temperature Outlier **(Bold Font)**

Temperature/°C	Temperature/K	VP_{expt}/Pa	VP_{calc}/Pa‡	Percent Difference*
0	273.15	0.6660	0.6660	0.00
20	**293.15**	**2.103**	**4.206**	**–50.00**
40	313.15	20.07	20.07	0.00
60	333.15	76.82	76.82	0.00
80	353.15	246.3	246.3	0.00
100	373.15	683.6	683.6	0.00
125	398.15	2076	2076	0.00
150	423.15	5435	5435	0.00
175	448.15	12610	12610	0.00
200	473.15	26470	26470	0.00

*100 • $(VP_{expt}-VP_{calc})/VP_{calc}$
‡Based on eq 1

3. RESULTS AND DISCUSSION

The three metrics addressed in this report are assessed by comparing how well they reproduce the fabricated data listed in Tables 1–3 and also comparing how they describe a real data set recently obtained for thiodiglycol. The comparisons were performed by minimizing the metrics, specifically, the sums of (1) the squares of the differences of experimental and correlated vapor pressures, (2) the squares of the differences of the natural logarithms of the experimental and correlated vapor pressures, and (3) the absolute values of the differences of the natural logarithms of the experimental and correlated vapor pressures, by adjusting the correlation coefficients. These metrics are referred to as difference squared, log-difference squared, and log-difference, respectively, in the following discussion.

3.1 Difference Squared Analysis of Vapor Pressure Data

As pointed out by Penski, summing the squares of the differences between experimental and correlated values weights the higher data values over the lower values and was discarded after attempting to correlate the data listed in Table 1.[13] We were unable to optimize this correlation for the data in Table 1 and abandoned it after observing that the optimization rapidly approached an unsatisfactory limit, that is, positive curvature of the standard plot as seen in Figure 1 and accompanying large positive *c* constant. As expected, data sets with lower-temperature outliers were affected less by including the outlier data points since this correlation weights higher values more than lower values.

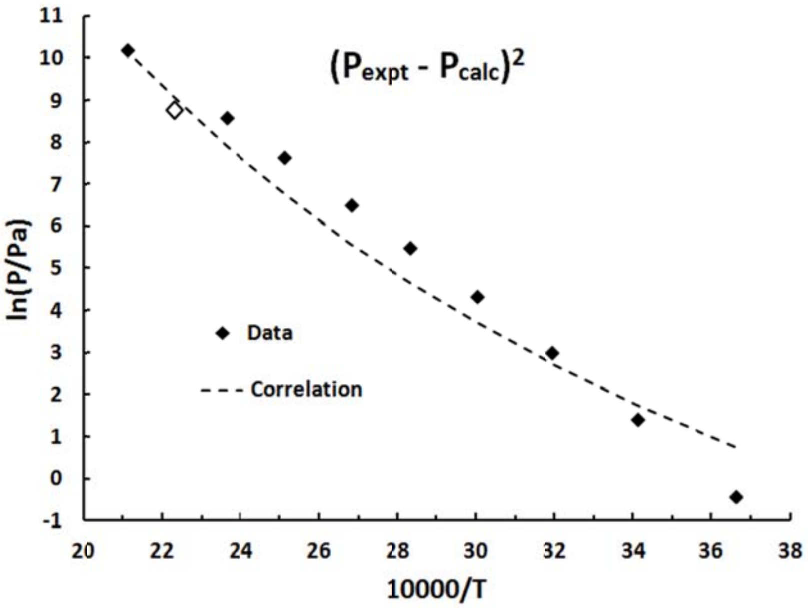

Figure 1. Difference Squared Analysis for Data (Diamonds) Containing High-Temperature Outlier (Open Diamond).

3.2 Log Difference Squared Analysis of Vapor Pressure Data

A log-difference squared analysis using the natural logarithms of the vapor pressure data was evaluated next. The fit was optimized using the Antoine equation and compared to the test data in Tables 1–3.

For the data in Table 1, with the outlier data point at 175 ºC, the resulting fit, shown in Figure 2, was satisfactory for the lower data, but to accommodate the outlier data, significantly underestimates the data points at 125, 150, and 200 ºC. Table 4 provides numeric values for the data illustrated in Figure 2. The resulting Antoine equation *c* value in Table 4, 74.4000, reflects the greater curvature of the plot shown in Figure 2 compared to eq 1 as a result of the influence of the outlier data point.

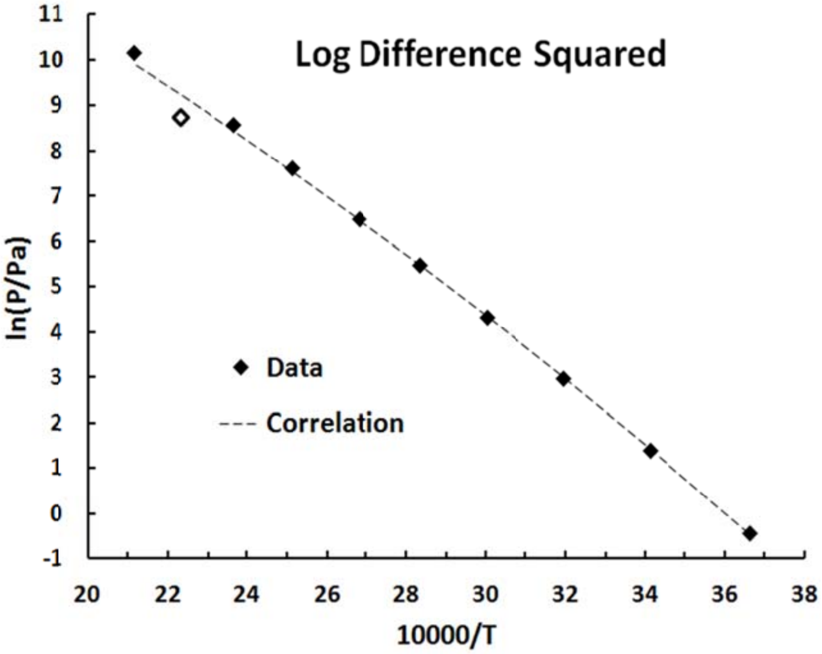

Figure 2. Log-Difference Squared Analysis for Data (Diamonds) Containing High-Temperature Outlier (Open Diamond).

Table 4. Optimized Correlation for Data Containing High-Temperature Outlier Using Log-Difference Squared Analysis

T/ºC	VP_{expt}	VP_{calc}	% Difference
0	0.666	0.651	2.30
20	4.206	4.302	–2.24
40	20.07	20.72	–3.15
60	76.82	78.27	–1.85
80	246.3	244.3	0.81
100	683.6	654.8	4.40
125	2076	1892	9.72
150	5435	4695	15.75
175	6302	10318	–38.92
200	26470	20542	28.86

$\ln(P/Pa) = 20.2249 – 4105/(T – 74.4000)$

A log-difference squared analysis for the data in Table 2, with outlier data point in the middle of the data set, is shown in Figure 3. This correlation resulted in a flattening of the correlation equation in an attempt to accommodate the outlier data, as evidenced by the lower absolute value of the *c* constant (-13.2551) compared to eq 1, shown at the bottom of Table 5, which also has the numeric values for the data shown in Figure 2.

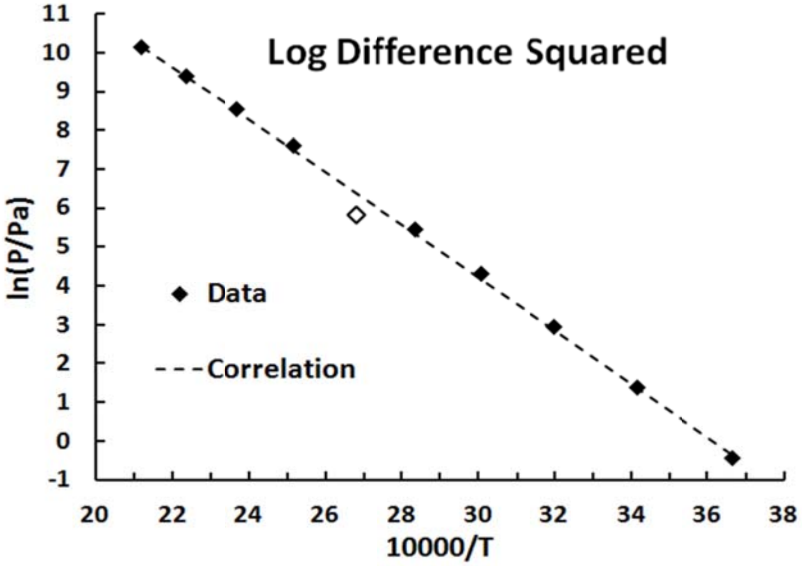

Figure 3. Log-Difference Squared Analysis for Data (Diamonds) Containing Mid-Temperature Outlier (Open Diamond).

Table 5. Optimized Correlation for Data Containing Mid-Temperature Outlier Using Log-Difference Squared Analysis

T/ºC	VP_{expt}	VP_{calc}	% Difference
0	0.6660	0.7227	–7.85
20	4.206	4.065	3.47
40	20.07	18.16	10.54
60	76.82	67.28	14.18
80	246.3	213.7	15.27
100	341.7	596.7	–42.74
125	2076	1854	11.98
150	5435	5018	8.31
175	12606	12109	4.10
200	26472	26554	–0.31

$$\ln(P/Pa) = 23.8466 - 6282/(T - 13.2551)$$

A log-difference squared analysis for the data in Table 3, with the outlier data point at the low end of the data, is shown in Figure 4. This data set resulted in a significant underestimation of the values at 0, 40, and 60 °C in an attempt to accommodate the 20 °C outlier data as seen in Figure 4 and Table 6. The *c* constant resulting from this analysis was more negative than the *c* value in eq 1, consistent with the greater curvature introduced by accommodating the outlier data point.

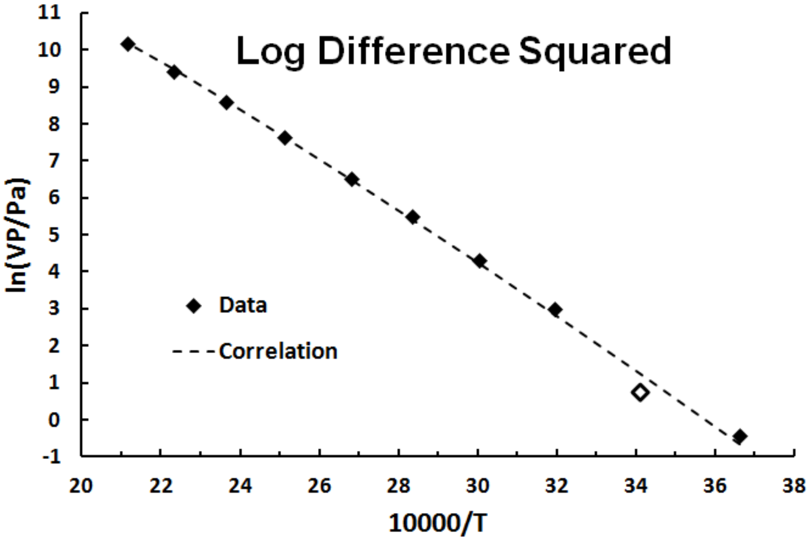

Figure 4. Log-Difference Squared Analysis for Data (Diamonds) Containing Low-Temperature Outlier (Open Diamond).

Table 6. Optimized Correlation for Data with Low-Temperature Outlier Using Log-Difference Squared Analysis

T/ºC	VP_{expt}	VP_{calc}	% Difference
0	0.666	0.5199	28.09
20	2.103	3.506	–40.01
40	20.07	17.59	14.11
60	76.82	69.98	9.78
80	246.3	231.3	6.46
100	683.6	658.1	3.87
125	2076	2048	1.34
150	5435	5465	–0.56
175	12610	12871	–2.03
200	26470	27361	–3.26

$\ln(P/Pa) = 22.0795 - 4961.50/(T - 54.9043)$

3.3 Log-Difference Analysis of Vapor Pressure Data

The next set of analyses was performed using the sum of the absolute values of the differences of the natural logs of the measured and correlated values, or log-difference, for data listed in Tables 1–3.

The resulting fit, shown in Figure 5, reproduced all of the values in Table 1 exactly with the exception of the outlier indicating that this fit to the data is not influenced by the outlier. Table 7 provides numeric values for the data illustrated in Figure 5. Further attempts to improve the correlation between measured and correlated data were unsuccessful.

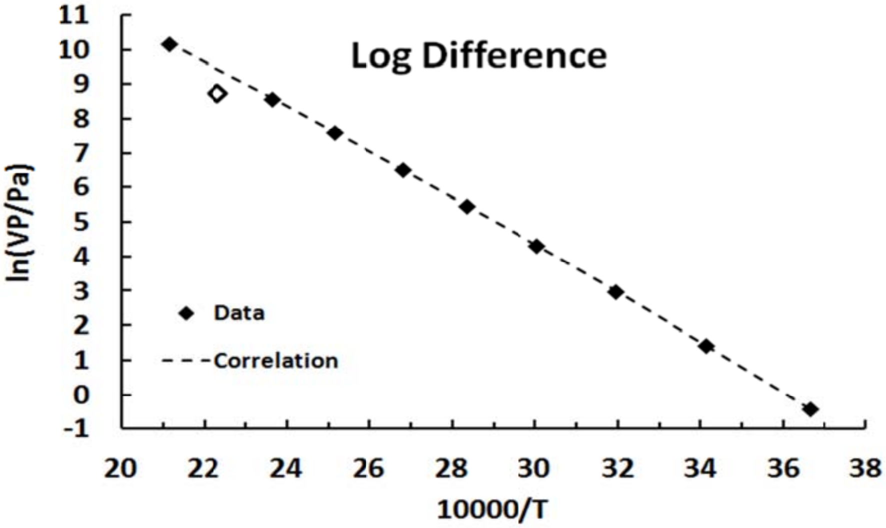

Figure 5. Log-Difference Analysis for Data (Diamonds) Containing High-Temperature Outlier (Open Diamond).

Table 7. Optimized Correlation and Data Containing High-Temperature Outlier Using Log-Difference Analysis

T/^{o}C	VP_{expt}	VP_{calc}	% Difference
0	0.6660	0.6660	0.00
20	4.206	4.206	0.00
40	20.07	20.07	0.00
60	76.82	76.82	0.00
80	246.3	246.3	0.00
100	683.6	683.6	0.00
125	2076	2076	0.00
150	5435	5435	0.00
175	6302	12606	–50.01
200	26472	26472	0.00

$\ln(P/Pa) = 22 - 5000/(T - 50.0000)$

For the data in Table 2, the log-difference analysis, shown in Figure 6, reproduced all of the measured data exactly with the exception of the outlier. This result is the same as that for the dataset with the high-temperature outlier. Table 8 provides numeric values for the data illustrated in Figure 6. Further attempts to improve the correlation between measured and correlated data were unsuccessful.

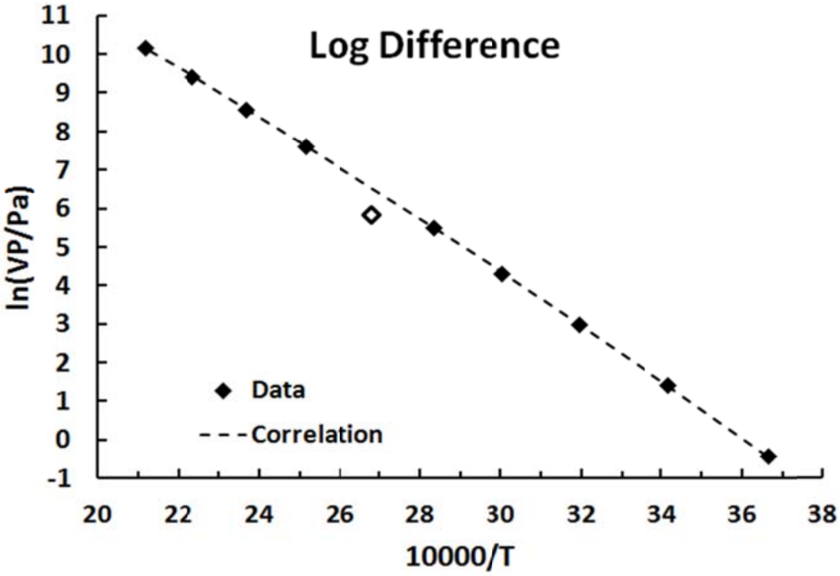

Figure 6. Log-Difference Analysis for Data (Diamonds) Containing Mid-Temperature Outlier (Open Diamond).

Table 8. Optimized Correlation for Data Containing Mid-Temperature Outlier Using the Log-Difference Analysis

T/ºC	VP_{expt}	VP_{calc}	% Difference
0	0.6660	0.6660	0.00
20	4.206	4.206	0.00
40	20.07	20.07	0.00
60	76.82	76.82	0.00
80	246.3	246.3	0.00
100	341.7	683.6	–50.01
125	2076	2076	0.00
150	5435	5435	0.00
175	12606	12606	0.00
200	26472	26472	0.00

$\ln(P/Pa) = 22.0000 - 5000.00/(T - 50.0000)$

For the data in Table 3, the fit using log-difference analysis, shown in Figure 7, reproduced all of the measured data exactly with the exception of the outlier. Table 9 provides numeric values for the data illustrated in Figure 7. Further attempts to improve the correlation between measured and correlated data were unsuccessful.

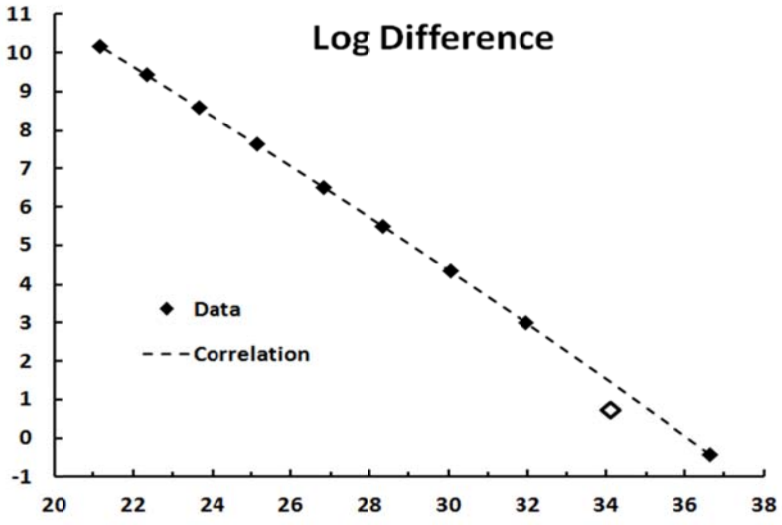

Figure 7. Log-Difference Analysis for Data (Diamonds) Containing Low-Temperature Outlier (Open Diamond).

Table 9. Optimized Correlation for Data Containing Low-Temperature Outlier Using the Log-Difference Analysis

T/ºC	VP_{expt}	VP_{calc}	% Difference
0	0.666	0.6660	0.00
20	2.103	4.206	–50.00
40	20.07	20.07	0.00
60	76.82	76.82	0.00
80	246.3	246.3	0.00
100	683.6	683.6	0.00
125	2076	2076	0.00
150	5435	5435	0.00
175	12610	12606	0.00
200	26470	26472	0.00

$\ln(P/Pa) = 22.0000 - 5000/(T - 50.0000)$

For correlation of experimental vapor pressure data using the Antoine equation, these results show conclusively that using the log-difference metric minimizes any correlation errors introduced by a single bad data value in a data set when compared to a log-difference squared analysis. The apparent explanation is that squaring the errant value over-emphasizes its influence on the correlation. Using the difference in logarithms mitigates this problem for data sets containing a single outlier data point, as shown above. This conclusion only applies to the situation where a single outlier is present and does not necessarily apply to cases where data contains random experimental variations. In practice, it is useful to identify outlier data points which can then be assessed regarding reliability and whether they should be included in the final analysis of such data.

Ongoing work on the vapor pressure of thiodiglycol (CAS No. 111-68-8) provides an example in which the log-difference squared metric appears to yield a more satisfactory result than the log-difference.[17] In that case, there is a wide temperature separation between data measured by vapor saturation and data measured by DSC. In addition, there were nearly twice as many useable data points measured by DSC than by vapor saturation. In that work, it was observed that the log-difference analysis produced calculated values for data at the low end of the temperature range with deviations from the experimental data as high as 10%. This value exceeds the expected error limits for the method, which are usually near 3% but can be as high as 5%. Using the log-difference squared metric in this case reduced the variances to 3-6% for each of the four vapor saturation data points and are deemed to be within the acceptable limits of this data set.

3.4 Correlating Liquid and Solid Phase Data Through the Melting Point

The phase change transition (melting point) has occurred within the range of experimental data in a number of recent investigations. In most cases where a phase change occurs, the data for each phase are treated separately, and no consideration of the transition is given other than in some cases to compare extrapolated melting points using the data measured for each phase. In the following, we provide a method to use all available information to quantitatively assess data above and below the melting point.

The slope of the standard vapor pressure plot is directly related to the heat of vaporization of the liquid phase and heat of sublimation of the solid phase by eqs 2 and 3, respectively.

$$\Delta H_{vap} = b_{liq} \cdot R \cdot (T/(c_{liq} + T))^2 \quad (2)$$

$$\Delta H_{sub} = b_{sol} \cdot R \cdot (T/(c_{sol} + T))^2 \quad (3)$$

where ΔH_{vap} is the enthalpy of vaporization of the liquid phase, ΔH_{sub} is the enthalpy of sublimation of the solid phase, b_{sol} and c_{sol} are Antoine equation constants for the solid phase correlation, b_{liq} and c_{liq} are Antoine equation constants for the liquid phase correlation, R is the gas constant, and T is absolute temperature. An example of this type of data set is shown in Figure 8 for a fabricated data set.

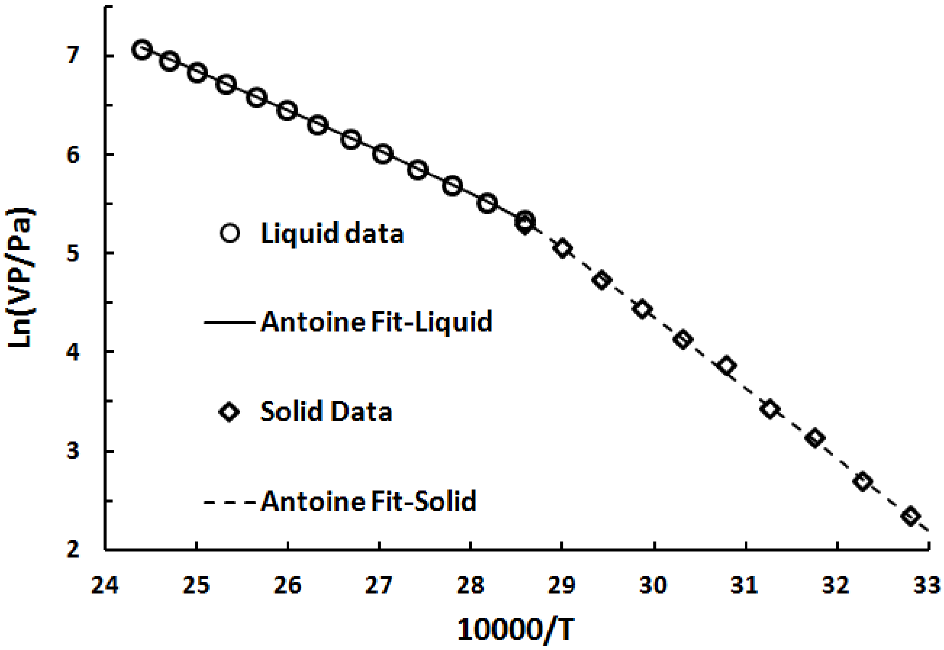

Figure 8. Example Vapor Pressure Data Set Spanning Phase Transition.

Since the difference between heat of vaporization and heat of sublimation at the melting point corresponds to the heat of fusion, eq 4, a change in the slope of the vapor pressure versus temperature graph is expected at the melting point.

$$\Delta H_{fus} \quad = \quad \Delta H_{sub} \quad - \quad \Delta H_{vap} \tag{4}$$

In a number of recent studies, the DSC method has been used to measure the vapor pressure of liquid phase chemicals while the vapor saturation method has been used to measure data for the same material in the solid phase. Examples include sulfur mustard[14] and EA 6095.[15] In cases where narrow temperature ranges are measured, a two-parameter correlation, that is, Clausius-Clapeyron, may be used unless a significant improvement is realized by using an Antoine equation correlation. For the present work, we will use a three-parameter Antoine equation correlation that may be simplified to a two-parameter, that is, $c = 0$, fit, if appropriate. We will treat the case where the heat of fusion is known or can be measured first.

If the heat of fusion is known or can be measured, that information is useful in determining the best correlation for data spanning the phase transition. If not, and the data are well populated, the heat of fusion can be inferred as before.[15] For the case where the heat of fusion is known, the following procedure has been developed:

As stated in eq 4, the difference between the heat of vaporization and heat of sublimation corresponds to the heat of fusion.

If the enthalpy of fusion and melting temperature (T_m) are known or can be measured, eq 5 may be derived from eqs 2–4.

$$\Delta H_{fus}/R \;=\; \Delta H_{sub}/R - \Delta H_{vap}/R \;=\; \boldsymbol{b}_{sol}\bullet(T_m/(\boldsymbol{c}_{sol} + T_m))^2 - \boldsymbol{b}_{liq}\bullet(T_m/(\boldsymbol{c}_{liq} + T_m))^2 \tag{5}$$

Solving eq 5 for b_{liq} produces eq 6.

$$b_{liq} \;=\; (b_{sol}\bullet(T_m/(c_{sol} + T_m))^2 - \Delta H_{fus}/R)/(T_m/(\boldsymbol{c}_{liq} + T_m))^2) \tag{6}$$

An additional assumption is that the vapor pressures of the liquid and solid phases are equal at the melting temperature. This assumption and the relationship between the respective Antoine constants are reflected in eq 7.

$$a_{sol} - b_{sol}/(c_{sol} + T_m) \;=\; a_{liq} - b_{liq}/(c_{liq} + T_m) \tag{7}$$

which can be solved for a_{liq} as shown in eq 8.

$$a_{liq} = \; a_{sol} - b_{sol}/(c_{sol} + T_m) \;+\; b_{liq}/(c_{liq} + T_m) \tag{8}$$

The correspondence between experimental and correlated data may be calculated using these equations, by assuming a starting value for c_{liq} and solving for a_{liq} (eq 8) and b_{liq} (eq 6) using the a_{sol}, b_{sol}, and c_{sol} constants determined from a fit of the solid data. An initial assessment of the data quality of each data set (liquid and solid), including which set has experimental data nearer to T_m, should be performed. In cases where the liquid data appear to be more reliable (and closer to T_m) than the solid data, the process described above can be reversed to calculate a_{sol} and b_{sol} based on the Antoine equation determined for the liquid data. The optimization process is performed by manually varying the c_{liq} (or c_{sol}) constant to obtain the best agreement between experimental and calculated values. In practice, it has been found that plotting the sum of the residual differences versus the constant allows the user to quickly identify the optimum set of correlation constants for a given data set.

In cases where there is insufficient experimental data to justify using a three-parameter fit, the calculation is simplified significantly since $c = 0$. In that case, we get eq 9, which can be rewritten in the more familiar form of eq 10.

$$\ln(\mathrm{VP}) = \Delta H_{vap}/RT + \text{constant} \tag{9}$$

$$\ln(\mathrm{VP/Pa}) = a - b/T_K \tag{10}$$

where VP is vapor pressure, ΔH_{vap} is the heat of vaporization, R is the gas constant, $\boldsymbol{a}$ and $\boldsymbol{b}$ are Clausius-Clapeyron equation correlation constants, and T_K is absolute temperature.

The heats of vaporization and sublimation are given by the product of the respective $\boldsymbol{b}$ coefficients, eqs 11 and 12, and by rearranging those equations, the difference between the solid $\boldsymbol{b}$ and liquid $\boldsymbol{b}$ is defined in eq 13.

$$\Delta H_{sub} = \boldsymbol{b}_{sol} \bullet R \tag{11}$$

$$\Delta H_{vap} = \boldsymbol{b}_{liq} \bullet R \tag{12}$$

$$\boldsymbol{b}_{sol} - \boldsymbol{b}_{liq} = (\Delta H_{sub} - \Delta H_{vap})/R = \Delta H_{fus}/R \tag{13}$$

where $\boldsymbol{b}_{sol}$ and $\boldsymbol{b}_{liq}$ are the solid and liquid Clausius-Clapeyron b coefficients, respectively, ΔH_{sub} is the heat of sublimation of the solid phase, ΔH_{vap} is the heat of vaporization of the liquid phase, and ΔH_{fus} is the heat of fusion.

Recognizing that the vapor pressure at the melting point is the same for the liquid and solid phases, eq 14 can be written and rearranged to eq 15.

$$a_{liq} - b_{liq}/T_m = a_{sol} - b_{sol}/T_m \tag{14}$$

$$a_{sol} - a_{liq} = (b_{sol} - b_{liq})/T_m = (\Delta H_{fus}/R)/T_m \tag{15}$$

where a_{sol} and a_{liq} are the solid and liquid Clausius-Clapeyron a coefficients, respectively.

At this point, a value of b_{sol} is chosen, fixing b_{liq} using eq 13, and a_{sol} is varied, fixing a_{liq} by eq 15, to minimize the sum of the absolute values of the difference between the natural logarithms of the observed and calculated vapor pressure values. This process is repeated using different b_{sol} values until the sum of the absolute percent differences is minimized.

4. CONCLUSIONS

Log-difference and log-difference squared analyses of vapor pressure data return reasonable fits to experimental data. Using the log-difference metric, as compared to the log-squared metric, reduces correlation error caused by a single bad data value. Since obvious outlier data are usually remeasured, ignored, rationalized away, or deleted without comment from real data sets, comparison or results using either metric can be useful. In the case of thiodiglycol, it has been found that the log-difference squared metric produces a more acceptable result than the log-difference metric since the variations between experimental and correlated values more closely conform to the known experimental uncertainties associated with data measurement.

A method has been described in detail that enables the user to correlate vapor pressure data spanning the phase transition temperature in the case where data exists on either side of the phase transition. This method takes advantage of all available information, especially heat of fusion, to minimize the metric of choice to quantitatively determine the best correlation of the experimental data.

LITERATURE CITED

1. Savage, J. J., Fielder, D. *The Vapor Pressure of Chemical Agents GD, VX, EA 2223, EA 3547, EA 3580, EA 5365, and EA 5533;* EC-TR-76058; Edgewood Arsenal: Aberdeen Proving Ground, MD, 1976; UNCLASSIFIED Report (AD-B013164).

2. Belkin, F., and Brown, H. A. *Vapor Pressure Measurements of Some Chemical Agents Using Differential Thermal Analysis, Part III;* EC-TR-75032; Edgewood Arsenal: Aberdeen Proving Ground, MD, 1975, UNCLASSIFIED Report (AD-A010666).

3. Smith, A., Menzies, A. W. C. Studies in Vapor Pressure: III. A Static Method of Determining the Vapor Pressures of Solids and Liquids. *J. Am. Chem. Soc.* **1910**, *32*, p 1412–1434.

4. *ASTM Standard Test Method for Vapor Pressure by Thermal Analysis*; ASTM E 1782-08; American Society for Testing and Materials International: West Conshohocken, PA.

5. Butrow, A. B., Seyler, R. J. Vapor pressure by DSC: extending ASTM E 1782 below 5 kPa. *Thermochim. Acta* **2003**, *402,* 145.

6. Brozena, A. Vapor pressure of 1-octanol below 5 kPa using DSC. *Thermochim. Acta* **2013**, *561,* 72–76.

7. *ASTM Standard Test Method for Vapor Pressure;* ASTM E 1194-07; American Society for Testing and Materials International: West Conshohocken, PA.

8. Buchanan, J. H.; Sumpter, K. B.; Abercrombie, P. L.; Tevault, D. E. *Vapor Pressure of GB;* ECBC-TR-686; U.S. Army Edgewood Chemical Biological Center: Aberdeen Proving Ground, MD, 2009; UNCLASSIFIED Report (AD-A500820).

9. Tevault, D. E., Brozena, A., Buchanan, J. H., Abercrombie-Thomas, P. L., Buettner, L. C. Thermophysical Properties of VX and RVX. *J. Chem. Eng. Data,* **2012**, *57,* 1970−1977.

10. Williams, B. R., M. S. Hulet, Brozena, A., Miles, Jr., R. W., Tevault, D. E. Vapor Pressure of 2-Dialkyl Aminoethanethiols. *J. Chem. Eng. Data,* **2013,** *58*, 1679−1684.

11. Butrow, A. B., Buchanan, J. H., Tevault, D. E. Vapor Pressure of Organophosphorus Nerve Agent Simulant Compounds. *J. Chem. Eng. Data*, **2009**, *54*, 1876–1883.

12. Tevault, D. E., Buchanan, J. H., Buettner, L. C., Matson, K. L. *Vapor Pressure of Cyclohexyl Methylphosphonofluoridate (GF).* ECBC-TR-304; U.S. Army Edgewood Chemical Biological Center: Aberdeen Proving Ground, MD, 2009; UNCLASSIFIED Report (AD-A503835).

13. Penski, E. C. *Vapor Pressure Analysis Methods, Statistics, and Applications*. CRDEC-TR-396; U.S. Army Chemical Research Development, and Engineering Center: Aberdeen

Proving Ground, MD, 1992; UNCLASSIFIED Report (AD-A255090). Penski, E. C., Latour, L. J., *Conversational Computation Method for Fitting the Antoine Equation to Vapor Pressure-Temperature Data. EATR-4491;* Edgewood Arsenal: Aberdeen Proving Ground, MD, 1971; UNCLASSIFIED Report (AD 881829).

14. Thomson, G. W. The Antoine Equation for Vapor-Pressure Data, *Chem. Rev.* **1946**, *38*, 1–39.

15. Buchanan, J. H., Buettner, L. C., Tevault D. E. Vapor Pressure of Solid Bis(2-chloroethyl) Sulfide, *J. Chem. Eng. Data* **2006**, *51,* 1331–1334.

16. Brozena, A., et al. Vapor Pressure of EA 6095, Journal of Chemical and Engineering Data, to be submitted, 2013.

17. Brozena, A., Tevault D. E., Irwin, K. Vapor Pressure of Thiodiglycol, Journal of Chemical and Engineering Data, to be submitted, 2013.


EDGEWOOD CHEMICAL BIOLOGICAL CENTER
A U.S. Army RDECOM Laboratory